

# Dalton Transactions

Accepted Manuscript



This is an *Accepted Manuscript*, which has been through the Royal Society of Chemistry peer review process and has been accepted for publication.

*Accepted Manuscripts* are published online shortly after acceptance, before technical editing, formatting and proof reading. Using this free service, authors can make their results available to the community, in citable form, before we publish the edited article. We will replace this *Accepted Manuscript* with the edited and formatted *Advance Article* as soon as it is available.

You can find more information about *Accepted Manuscripts* in the [Information for Authors](#).

Please note that technical editing may introduce minor changes to the text and/or graphics, which may alter content. The journal's standard [Terms & Conditions](#) and the [Ethical guidelines](#) still apply. In no event shall the Royal Society of Chemistry be held responsible for any errors or omissions in this *Accepted Manuscript* or any consequences arising from the use of any information it contains.



Journal Name

ARTICLE

# Controllable assembly, characterization and catalytic property of a new Strandberg-type organophosphotungstate

Received 00th January 20xx,  
Accepted 00th January 20xx

DOI: 10.1039/x0xx00000x

www.rsc.org/

Hong-Xin Ma,<sup>a</sup> Jing Du,<sup>a</sup> Fang Su,<sup>\*a,b</sup> Ting Lu,<sup>a</sup> Zai-Ming Zhu,<sup>\*a</sup> Lan-Cui Zhang<sup>\*a</sup>

Using phenylphosphonic acid, simple tungstate and copper(II) compound as starting materials, an organic-inorganic hybrid Strandberg-type organophosphotungstate,  $\{[(\text{Cu}(\text{H}_2\text{O})(\mu\text{-bipy}))_2(\text{C}_6\text{H}_5\text{PO}_3)_2\text{W}_5\text{O}_{15}]\}_n$  (bipy = 4,4'-bipyridyl) (**1**), was assembled successfully under hydrothermal condition and characterized by physico-chemical and spectroscopic methods. Compound **1** represents the first example of transition metal complex modified organophosphotungstate cluster. In the crystal structure of compound **1**, the polymeric 1-D  $\{\text{Cu-bipy}\}_n$  chains are interconnected by  $[(\text{C}_6\text{H}_5\text{PO}_3)_2\text{W}_5\text{O}_{15}]^{4-}$  (Abbreviated as  $\{(\text{C}_6\text{H}_5\text{P})_2\text{W}_5\}$ ) units into a 3-D framework. A hollow Keggin isopolytungstate  $[\text{H}_2\text{W}_{12}\text{O}_{40}]^{6-}$  ( $\{\text{W}_{12}\}$ )-Cu(II) coordination polymer,  $\{[\text{Cu}(\text{bipy})_2(\mu\text{-bipy})\text{Cu}(\text{bipy})_2(\text{H}_2\text{W}_{12}\text{O}_{40})]\cdot 12\text{H}_2\text{O}\}_n$  (**2**), was obtained at different molar ratio of the starting materials and pH. The two Cu(II) coordination polymers exhibit good acid-catalytic activity for the synthesis of cyclohexanone ethylene ketal. Their fluorescence properties were studied.

## Introduction

Organic or organometallic compounds, such as organosilicon, organophosphorus, and organotin, can be grafted on the polyanions, forming many new polyoxometalate (POM)-based hybrid materials.<sup>1</sup> Indeed, organic components are not only used as structure-directing agents in preparing many materials, but also can be directly embedded into the inorganic skeleton of the materials.<sup>2</sup> So far, a few works about POMs containing organophosphorous (RP) group have been reported already.<sup>1f,2,3</sup> Especially, a RP group as a central unit has been introduced into the strandberg-type POM skeleton successfully.<sup>2b,3d,3e,4</sup> However, most of POM-RP compounds are organophosphomolybdate  $\{(\text{RP})_2\text{Mo}_5\}$  series, the organophosphotungstate  $\{(\text{RP})_2\text{W}_5\}$  series have been rarely reported. As far as we know, only one example of strandberg-type polyoxotungstate with the central RP, *i.e.*,  $\{(\text{C}_4\text{H}_9)_3\text{NH}\}_4[(\text{C}_6\text{H}_5\text{PO}_3)_2\text{W}_5\text{O}_{15}]$  (Abbreviated as TBA- $(\text{C}_6\text{H}_5\text{P})_2\text{W}_5$ ), was synthesized by Pope in 1990.<sup>5</sup> While the strandberg-type  $\{(\text{RP})_2\text{W}_5\}$  derivative with transition metal complex modified or extended structure has not been reported so far. Our recent research work shows that the strandberg-type  $\{(\text{RP})_2\text{Mo}_5\}$  POMs,  $\{[\text{Cu}(\text{H}_2\text{O})_2(\mu\text{-bipy})_2(\text{C}_6\text{H}_5\text{PO}_3)_2\text{Mo}_5\text{O}_{15}]\}_n$  (Abbreviated as bipy-Cu- $(\text{C}_6\text{H}_5\text{P})_2\text{Mo}_5$ )

and  $\{[\text{Cu}(\text{H}_2\text{O})_2(\mu\text{-bipy})(\text{C}_6\text{H}_5\text{PO}_3)_2\text{Mo}_5\text{O}_{15}]\}_n$ , exhibit better catalytic activities than those of  $\{\text{P}_2\text{Mo}_5\}$  POMs with the centre inorganic phosphorus atoms,<sup>2c</sup> suggesting that the RP group play an important role in the catalytic activity of strandberg-type POM. In addition, this also shows that the strandberg-type POMs, as small molecules of the POM family, may have unpredictable properties and potential applications. Some performances, such as catalytic property, photoluminescence of the inorganic-organic hybrid POM materials can be enhanced after the introduction of transition metal and organic component into the structure.<sup>2c</sup> Through a variety of experiments, we found that the synthesis of the  $\{(\text{RP})_2\text{W}_5\}$  series is more difficult than that of the  $\{(\text{RP})_2\text{Mo}_5\}$  series. Therefore, the design of transition metal complex modified  $\{(\text{RP})_2\text{W}_5\}$  hybrids is a meaningful and challenging work. Herein, a new crystalline 3-D Cu (II) coordination polymer composed of 4,4'-bipy units and strandberg-type organophosphotungstate  $[(\text{C}_6\text{H}_5\text{PO}_3)_2\text{W}_5\text{O}_{15}]^{4-}$  polyanions was successfully synthesized by changing the synthetic conditions. And another Cu(II) coordination polymer containing Keggin isopolytungstate  $[\text{H}_2\text{W}_{12}\text{O}_{40}]^{6-}$  anion and 4,4'-bipy unit was unexpectedly obtained. The influence of the molar ratio of the starting materials, and pH of the mixture during the preparation of the crystalline structure was discussed detailedly. Additionally, the solid-state fluorescence property and catalytic activity of the compounds were also studied.

<sup>a</sup> School of Chemistry and Chemical Engineering, Liaoning Normal University, Dalian 116029, China. E-mail: zhanglancai@lnnu.edu.cn; chemzhu@sina.com; Fax: +86 41182158559; Tel: +86411 82156550.

<sup>b</sup> Centre of Analytical Test, Liaoning Normal University, Dalian 116029, China. E-mail: sufang861218@163.com.

† Electronic Supplementary Information (ESI) available: ORTEP views of compounds **1** and **2**; IR, XRPD, TG-DTA, Emission spectra and catalytic results. CCDC reference numbers: 1417285 and 1417286. For ESI and crystallographic data in CIF or other electronic format. See DOI:10.1039/b000000x/

## Experimental

### Reagents and general methods

All reagents were commercially available and were used as received. TBA- $(\text{C}_6\text{H}_5\text{P})_2\text{W}_5$  was prepared and characterized

according to the reported procedures.<sup>5</sup> Elemental analyses were analysed on a Vario Elcube elemental analyzer (C, H and N) and a Prodigy XP emission spectrometer (P, Cu and W). Single crystal X-ray diffraction data were collected on a Bruker Smart APEX IIX-diffractometer equipped with graphite-monochromated Mo K $\alpha$  radiation ( $\lambda = 0.71073 \text{ \AA}$ ). The infrared spectra (IR) were recorded on KBr pellets with a Bruker AXS TENSOR-27 FTIR spectrometer in the range of 4000-400  $\text{cm}^{-1}$ . X-ray powder diffraction (XRPD) data were obtained on a Bruker AXS D8 Advance diffractometer using Cu K $\alpha$  radiation ( $\lambda = 1.5418 \text{ \AA}$ ) with a step size of  $0.02^\circ$  in the  $2\theta$  range from  $5$  to  $60^\circ$ . Thermal analyses (TGA-DTA) were carried out on a Pyris Diamond TG-DTA thermal analyzer in air at a heating rate of  $10^\circ\text{C min}^{-1}$ . The solid UV spectra were performed on a Perkin-Elmer Lambda 35 UV-Visible spectrophotometer. The photoluminescence property was determined on a HITACHI F-7000 fluorescence spectrophotometer in the solid state at room temperature. The yield of cyclohexanone ethylene ketal was confirmed on a JK-GC112A Gas Chromatograph.

### Synthesis of compounds

**Compound 1.**  $\text{CuCl}_2 \cdot 2\text{H}_2\text{O}$  (0.03 g, 0.18 mmol) and  $\text{Na}_2\text{WO}_4 \cdot 2\text{H}_2\text{O}$  (0.18 g, 0.54 mmol) were dissolved in 20 mL of distilled water under stirring at room temperature for 20 min. Then  $\text{C}_6\text{H}_5\text{PO}_3\text{H}_2$  (0.10 g, 0.64 mmol) was added to the above solution under stirring, and the pH of the mixture was adjusted to 2-3 with 4 mol  $\text{L}^{-1}$  HCl. Finally, bipy (0.05 g, 0.32 mmol) was added. The resulting mixture was transferred to a 30 mL Teflon-lined autoclave and kept at  $150^\circ\text{C}$  for 3 days, blue block crystals were isolated (yield: ca. 40% based on W). Elemental analysis, Calc. for  $\text{C}_{32}\text{H}_{30}\text{O}_{23}\text{N}_4\text{Cu}_2\text{P}_2\text{W}_5$ : C 19.7, H 1.55, N 2.9, P 3.2, Cu 6.5, W 47.2%; Found: C 19.65, H 1.6, N 3.0, P 3.1, Cu 6.4, W 47.2%. IR (KBr pellet),  $\text{cm}^{-1}$ : 3447(w), 3115(m), 1613(m), 1530(w), 1408(m), 1313(w), 1223(w), 1160(m), 1128(s), 1033(m), 964(m), 939(s), 887(s), 812(m), 722(s), 686(s), 560(m), 512(m).

**Compound 2.**  $\text{CuCl}_2 \cdot 2\text{H}_2\text{O}$  (0.09 g, 0.54 mmol) and  $\text{Na}_2\text{WO}_4 \cdot 2\text{H}_2\text{O}$  (0.18 g, 0.54 mmol) were dissolved in 20 mL of distilled water under stirring at room temperature for 20 min. Then  $\text{C}_6\text{H}_5\text{PO}_3\text{H}_2$  (0.10 g, 0.64 mmol) was added to the above solution under stirring, and the pH of the mixture was adjusted to 3-4 with 4 mol  $\text{L}^{-1}$  HCl. Finally, bipy (0.15 g, 0.96 mmol) was added. The resulting mixture was transferred to a 30 mL Teflon-lined autoclave and kept at  $150^\circ\text{C}$  for 3 days, Blue block crystals were obtained (yield: ca. 32% based on W). Elemental analysis, Calc. for  $\text{C}_{60}\text{H}_{74}\text{O}_{52}\text{N}_{12}\text{Cu}_3\text{W}_{12}$ : C 17.2, H 1.8, N 4.0, Cu 4.5, W 52.6%; Found: C 17.3, H 1.9, N 4.1, Cu 4.5, W 52.8%. IR (KBr pellet),  $\text{cm}^{-1}$ : 3456 (m), 3136(m), 1614(m), 1399(s), 1222(w), 1134(w), 919(w), 864(w), 775(m), 632(w).

### Single-crystal X-ray crystallography

The structures were solved by direct methods and refined by full-matrix least-squares fitting on  $F^2$  using SHELXTL-2014 package. An empirical absorption correction was applied using the SADABS program.<sup>6,7</sup> Crystal data and structure refinement parameters of compounds **1** and **2** were listed in Table 1. H atoms on C atoms were added in calculated positions. In compound **2**, eleven lattice water molecules could be

Table1 Crystal and Refinement Data for **1** and **2**

	<b>1</b>	<b>2</b>
Formula	$\text{C}_{32}\text{H}_{30}\text{O}_{23}\text{N}_4\text{Cu}_2\text{P}_2\text{W}_5$	$\text{C}_{60}\text{H}_{74}\text{O}_{52}\text{N}_{12}\text{Cu}_3\text{W}_{12}$
Formula weight	1946.87	4192.04
T/K	296(2)	296(2)
Wavelength/ $\text{\AA}$	0.71073	0.71073
Crystal system	Orthorhombic	Monoclinic
Space group	<i>Fdd2</i>	<i>P2<sub>1</sub>/c</i>
<i>a</i> / $\text{\AA}$	19.0050(11)	12.796(4)
<i>b</i> / $\text{\AA}$	42.763(2)	25.625(7)
<i>c</i> / $\text{\AA}$	10.6834(6)	16.112(3)
$\alpha/^\circ$	90.00	90
$\beta/^\circ$	90.00	119.955(16)
$\gamma/^\circ$	90.00	90
<i>V</i> / $\text{\AA}^3$ , <i>Z</i>	8682.6(9), 8	4577(2), 2
<i>D<sub>c</sub></i> /g $\text{cm}^{-3}$ , <i>F</i> <sub>000</sub>	2.979, 7136	3.042, 3816
GOF	1.082	1.047
Reflections collected	10739	22894
Unique data, <i>R</i> <sub>int</sub>	3340, 0.0358	8059, 0.0372
$\theta$ Range( $^\circ$ )	1.905 to 24.995	1.661 to 25.00
<i>R</i> <sub>1</sub> ( <i>I</i> > 2 $\sigma$ ( <i>I</i> )) <sup>o</sup>	0.0238	0.0854
<i>wR</i> <sub>2</sub> (all data) <sup>o</sup>	0.0625	0.1965

$$^o R_1 = \sum ||F_o| - |F_c|| / \sum |F_o|; wR_2 = \sum [w(F_o^2 - F_c^2)^2] / \sum [w(F_o^2)^2]^{1/2}$$

accurately assigned from the residual electron peaks, another one lattice water molecule was directly included in the molecular formula based on the elemental analysis and TG analysis. All hydrogen atoms on water molecules were directly included in the final molecular formula. The selected bond lengths and angles, and hydrogen bonds are listed in Tables S1-S3. † CCDC reference numbers: 1417285 and 1417286.

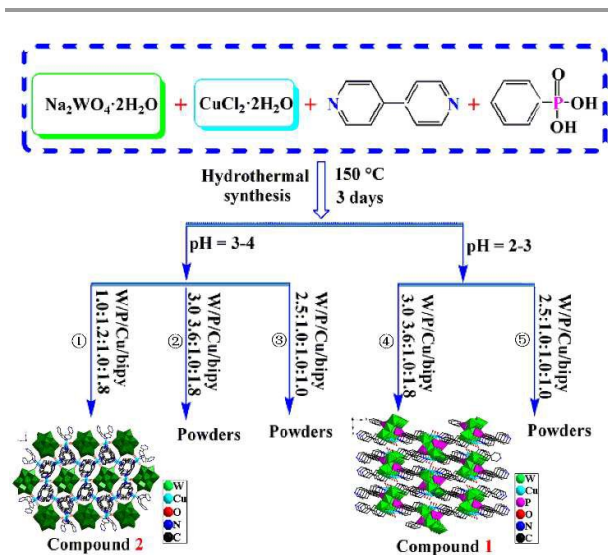
### Catalytic experiment

Following the method mentioned in our previous work,<sup>1f,2c</sup> the typical procedure for the acid catalytic synthesis is: the catalyst (e.g. compound **1**) was added to a mixture of cyclohexanone, glycol and 10 mL of cyclohexane in a 100 mL three-necked round-bottom flask fitted with a Dean-Stark apparatus to remove the water continuously from the reaction mixture. For the insoluble catalyst, the catalytic reaction undergoes a heterogeneous process, after completing the reaction, the catalyst could be separated from the organic phase containing product through decantation. Furthermore, the reusabilities of compounds **1** and **2** were studied through three cycles under the optimum reaction conditions. The obtained ketal products were tested by gas chromatography.

## Results and discussion

### Synthesis

The organophosphorus group, as a central unit, is difficult to be introduced into the POM system because of the hydrophobicity of the organic components and the spatial configuration of a POM, although some  $\{(\text{RP})_2\text{Mo}_5\}$  compounds have been obtained. In particular, the preparation of  $\{(\text{RP})_2\text{W}_5\}$  series is more difficult. Moreover, it is another challenge to harvest the crystals and further determine their structures. According to the synthetic methods of bipy-Cu-( $\text{C}_6\text{H}_5\text{P}$ )<sub>2</sub>Mo<sub>5</sub>



**Scheme 1** Schematic diagram of the pH-, the molar ratio-controlled assembly process of compounds **1** and **2**

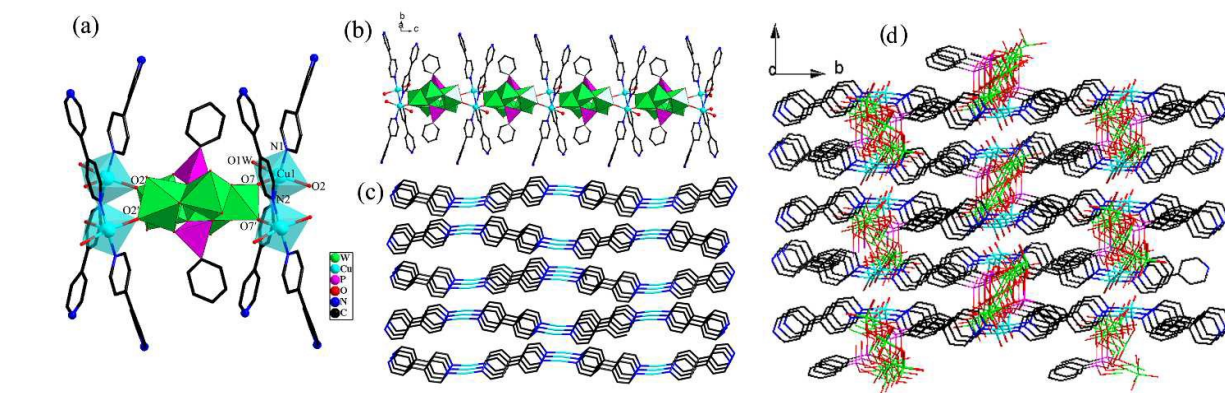


**Fig. 1** (a) Structural representation of the coordination environment of four Cu(II) ions around the strandberg-type  $\{(C_6H_5P)_2W_5\}$  cluster in **1**; (b) The 1-D chain of  $\{(C_6H_5P)_2W_5\}$  units linked by Cu-bipy/ $H_2O$  fragments along  $c$  axis in **1**; (c) Wire representation of the polymeric 1-D chains of  $\{Cu-bipy\}_n$  along the  $b$  axis (H and polyanions have been omitted for clarity); (d) Wire representation of a 3-D structure of **1**

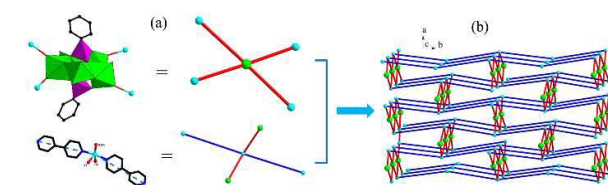


**Fig. 2** (a) Perspective views of the four-connected (Cu atom and  $\{(C_6H_5P)_2W_5\}$  polyanion) nodes in compound **1**. Blue dashed lines illustrate the four-connected circumstances of Cu atom; (b) Schematic representation of the bimodal four-connected 3D net of  $(4.6^4.8)_2(4^2.6^2.8^2)$  topology (H atoms are omitted for clarity)

### Structural analysis

Single crystal X-ray diffraction analysis reveals that compound **1** and bipy-Cu- $\{(C_6H_5P)_2Mo_5\}$  are isostructural. The main structural characteristics of **1** is also considered as Cu(II) coordination polymer, and consists of  $[(C_6H_5PO_3)_2W_5O_{15}]^{4-}$  polyanions and  $[(Cu(H_2O))_2(\mu-bipy)_2]^{4+}$  cations, the asymmetrical unit of **1** is shown in Fig. S1a.† The  $\{(C_6H_5P)_2W_5\}$  unit acts as a tetradentate ligand and coordinates to four  $Cu^{2+}$

reported in our recent work,<sup>2c</sup> the similar synthetic protocol was adopted except that  $Na_2WO_4$  was used in place of  $Na_2MoO_4$  in order to obtain the crystalline bipy-Cu(II) modified strandberg-type organophosphotungstate. In the identical conditions, *i.e.*, the molar ratio of W/P/Cu/bipy is 2.5: 1.0: 1.0: 1.0, pH is 3-4 (Scheme 1, step③), unfortunately, only powders were obtained. When the molar ratio of W/P/Cu/bipy was increased to 3.0: 3.6: 1.0: 1.8 (Step ②), no crystal was gained. While attempting to decrease the molar ratio of W/P to 1.0: 1.2 (step①), the blue block crystal (compound **2**) was got unexpectedly, the RP group has not been introduced into the POM skeleton. In order to probe the effect of the pH, according to the protocol of step ③, only the pH was changed from 3-4 to 2-3 (step ⑤), no crystal was obtained. Keeping the molar ratio of the starting materials as step ②, and the pH was adjusted to 2-3, the blue block crystals were isolated (compound **1**) was successfully harvested (step ④). The above results indicate that the  $\{(C_6H_5P)_2W_5\}$  compounds, compared with  $\{(C_6H_5P)_2Mo_5\}$  series, are more sensitive to the reaction conditions, such as pH and the molar ratio of the precursors.

ions *via* four terminal oxygen atoms (O2/O2', O7/O7') (Fig. 1a), and the symmetrical Cu1 is five-coordinate with two N atoms (N1, N2) from two bipy ligands, two terminal oxygen atoms (O2, O7), and one terminal water ligand (O1W), to give a square-pyramid configuration. The bond lengths of Cu1–O2, Cu1–O7, Cu1–N1, Cu1–N2 and Cu1–O1W are 1.961(9), 2.363(9), 2.008(10), 2.035(10) and 1.963(10) Å, respectively. The W–O distances are in the normal range (1.705(9)–2.395(8) Å) (Table S1†). As shown in Fig. 1b, the adjacent two  $\{(C_6H_5P)_2W_5\}$  units are linked by two symmetrical  $Cu^{2+}$  ( $Cu1/Cu1'$ ) ions, forming an infinite 1-D chain stretching along  $c$  axis. Obviously, the  $Cu^{2+}$  ions not only link  $\{(C_6H_5P)_2W_5\}$  units, but also connect bipy ligands, to generate polymeric 1-D  $\{Cu-bipy\}_n$  chains parallel to the  $b$  axis (Fig. 1c), with adjacent chains are interconnected by polyoxoanions into a 3-D framework through coordination bonding and hydrogen bonding interactions (Fig. 1d). The hydrogen bonds of O1W–H1WA...O5 and O1W–H1WB...O8 are 2.707(13) and 2.671(12)



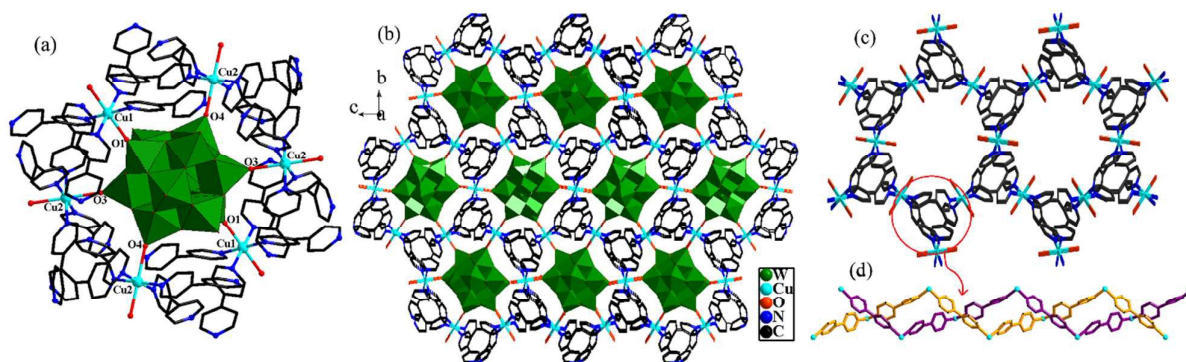


**Fig. 3** (a) Structural representation of the coordination environment of six Cu(II) ions around the  $[H_2W_{12}O_{40}]^{6-}$  polyanion in **2**; (b) Polyhedral and stick representation of a 3-D structure of **2**; (c) Stick representation of  $\{Cu\text{-}bipy\}_n$ ; (d) Ball and Stick representation of two intertwined chains constructed by  $\{Cu\text{-}bipy\}_n$  around the periphery of polyanion clusters (The H and polyanions have been omitted for clarity)

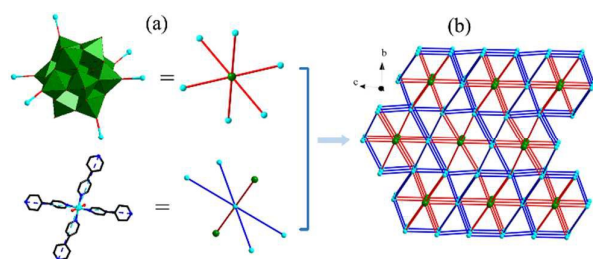


**Fig. 4** (a) Perspective views of the six-connected (Cu atom and  $\{W_{12}\}$  polyanion) nodes in compound **2**. Blue dashed lines illustrate the six-connected circumstances of Cu atom. (b) Schematic representation of the bimodal six-connected 3D net of  $(4^6.5^5.6^2.7^2)_3(4^6.5^6.7^3)$  topology

$\text{\AA}$  (Table S2<sup>†</sup>), respectively. The 3-D network topology of compound **1** can be further described as Fig. 2. In this simplification, the Cu atoms act as one kind of the four-node  $(4.6^4.8)$ , and the  $\{(C_6H_5P)_2W_5\}$  unit acts as the other  $(4^2.6^2.8^2)$  (Fig. 2a). From the topological point of view, the 3-D structure of compound **1** can be simplified to a unique bimodal four-connected 4,4-c net with stoichiometry  $(4-c)(4-c)_2$  and the point symbol for the net is  $(4.6^4.8)_2(4^2.6^2.8^2)$  (Fig. 2b).

For the structure unit of **2**, as shown in Figs. 3 and S1b<sup>†</sup>, each molecular unit is composed of one distort metatungstate  $[\alpha\text{-}H_2W_{12}O_{40}]^{6-}$  polyanion, two Cu-bipy complex fragments and twelve crystal water molecules. The four central  $\mu\text{-O}$  atoms of  $\{W_{12}\}$  are disordered over eight positions with each oxygen site half-occupied. Each  $\{W_{12}\}$  coordinates to six  $Cu^{2+}$  ions *via* six terminal oxygen atoms (O1/O1', O3/O3', O4/O4') acting as a hexadentate ligand (Fig. 3a). Two crystallographically independent Cu(II) ions have similar coordination environments. The Cu1/Cu2 center coordinate with two  $WO_6$  octahedral oxygen atoms from two polyanion units, four nitrogen atoms from two bipy ligands. The Cu–O bond lengths are 2.308(17), 2.308(17) for Cu1 and 2.446(16), 2.478(17)  $\text{\AA}$  and for Cu2, respectively, and the Cu–N distances are in the range of 2.02(2)–2.15(2) and 2.04(2)–2.09(2)  $\text{\AA}$  for Cu1 and Cu2, respectively (Table S3<sup>†</sup>). A 3-D architecture is also constructed through coordination and hydrogen bonding interactions (Fig. 3b). As shown in Fig. 3b, each  $\{W_{12}\}$  cluster is surrounded by six  $\{Cu\text{-}bipy\}$  clusters, and each  $\{Cu\text{-}bipy\}$  cluster actually consists

of two intertwined chains (Figs. 3c and d). From the topological viewpoint, the Cu atom can be reduced to a six-connection node, and the  $\{W_{12}\}$  polyanion acts as one kind of a six-connected node. The final net is a two-nodal six-connected 6,6-c net with stoichiometry  $(6-c)(6-c)_3$ . The extended point symbol is  $(4.4.4.4.4.4.5.5.5.5.5.2.6_4.6_4.7_2.7_2)$  for the Cu node and  $(4.4.4.4.4.4.5_2.5_2.5_2.5_2.5_2.5_2.7_{16}.7_{16}.7_{16})$  for bimodal four-connected 4,4-c net with stoichiometry  $(4-c)(4-c)_2$  and the point symbol for the net is  $(4.6^4.8)_2(4^2.6^2.8^2)$   $\{W_{12}\}$  polyanion node (Fig. 4a), thus giving a short point symbol for net  $(4^6.5^5.6^2.7^2)_3(4^6.5^6.7^3)$  topology (Fig. 4b).

#### Characterizations

**IR spectroscopy.** The IR spectra of **1** and **2** are shown in Fig. S2.† For compound **1**, the peaks at 3447 and 3115  $\text{cm}^{-1}$  are attributed to the characteristic vibrations of O–H and N–H. The bands in the 1160–1033  $\text{cm}^{-1}$  region are due to  $\nu(\text{P–O})$  vibration of the organophosphorus. And the bands at 1613–1223  $\text{cm}^{-1}$  are associated with the pyridine ring of a bipy molecule.<sup>2c</sup> The characteristic bands at 964 and 939  $\text{cm}^{-1}$  are belong to  $\nu(W\text{–}O_{\text{terminal}})$ , and 887–560  $\text{cm}^{-1}$  are believed to be  $\nu(W\text{–}O_{\text{bridging}})$ , respectively.<sup>8</sup> As for compound **2**, the characteristic vibrations of Keggin unit appear at 919, 864 and 775  $\text{cm}^{-1}$   $\nu(W\text{–}O_{\text{terminal}})$  and  $\nu(W\text{–}O_{\text{bridging}})$ , respectively. No  $\nu(\text{P–O})$  vibration illustrates that the polyanion is a hollow Keggin structure. The strong bands at 1614, 1399 and 1222  $\text{cm}^{-1}$  are characteristic vibrations of bipy, and the bands at 3456 and 3136  $\text{cm}^{-1}$  are due to O–H and N–H vibrations.<sup>2c</sup>

**XRPD.** The XRPD patterns of compounds **1** and **2** as well as their simulated XRPD patterns are shown in Fig. S3.† The diffraction peaks on the patterns correspond well in position, confirming that the product is a pure phase. The differences in reflection intensity are probably due to preferred orientation in the powder samples.

**TGA-DTA.** To study the thermal stability of compounds **1** and **2**, their thermal behaviours were investigated using thermal analysis methods. TG and DTA analyses of **1** and **2** are given in Fig. S4.† From Fig. S4a,† it is found that the TG curve of compound **1** displays a three-continuous weight loss. The total weight loss of 26.11% (calc. 25.82%) in the temperature range

Table 2 Catalytic performances of **1** and **2** compared with the reference catalysts for the synthesis of cyclohexanone ethylene ketal

Entry	Catalyst	Solubility	Time (h)	Yield (%)
1	—	—	3.5	9
2	<sup>a</sup> CuCl <sub>2</sub>	soluble	3.5	~100
3	<sup>a</sup> TBA-(C <sub>6</sub> H <sub>5</sub> P) <sub>2</sub> W <sub>5</sub>	insoluble	3.5	73
4	<sup>b</sup> bipy-Cu-(C <sub>6</sub> H <sub>5</sub> P) <sub>2</sub> Mo <sub>5</sub>	insoluble	2.5	94
5	<sup>a</sup> Compound <b>1</b>	insoluble	3.5	95
6	<sup>a</sup> Compound <b>2</b>	insoluble	3.5	91

Reaction conditions: the molar ratio of cyclohexanone to glycol was 1: 1.4 (0.1 mol of cyclohexanone); water-carrying agent: 10 mL of cyclohexane; reaction temperature: 95-100 °C. a, b: the molar ratios of the catalyst to cyclohexanone are 1: 350 and 1: 200, respectively.

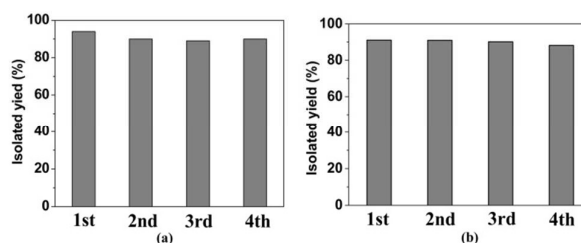
of 35-550 °C corresponds to the losses of two coordinate water molecules, two bipy molecules and two phenyl groups. Two exothermal peaks observed at 400 and 482 °C in the DTA curve are assigned to the combustion of the phenyl groups and bipy molecules, which means that the skeleton of Strandberg POM retain below 550 °C. For compound **2**, a two-continuous weight loss step is observed (Fig. S4b<sup>†</sup>). The total weight loss of 28.25% (calc. 27.51%) at the temperature 37-530 °C is attributed to the losses twelve water molecules, two H<sup>+</sup> ions and six bipy ligands. One exothermal peak observed at 515 °C in the DTA curve is assigned to the combustion of the bipy molecules. The above results show that compounds **1** and **2** have good thermal stabilities.

#### Solid UV-vis absorption spectra

In order to further understand optical properties of two compounds, the solid UV-vis absorption spectra of **1**, **2**, parent compound TBA-(C<sub>6</sub>H<sub>5</sub>P)<sub>2</sub>W<sub>5</sub> and bipy, between 200 to 800 nm, were presented in Fig. S5.<sup>†</sup> As seen from Figs. S5c-5d,<sup>†</sup> the parent compound TBA-(C<sub>6</sub>H<sub>5</sub>P)<sub>2</sub>W<sub>5</sub> and bipy have strong bands only in the UV region (227 nm and 260 nm), while two inorganic-organic hybrid title compounds show strong bands in the UV region and visible region (Figs. S5a-5b<sup>†</sup>). The absorption bands in the UV range of compounds **1** and **2** were assigned to a charge-transfer transition from the O→W and characteristic absorption of bipy.<sup>1†</sup> While the absorption bands at the visible region near to infrared region is due to the d-d transition coming from the introduction of the transition metal Cu<sup>2+</sup>.

#### Solid-state fluorescence properties

The solid-state luminescence properties of **1**, **2**, the parent compound TBA-(C<sub>6</sub>H<sub>5</sub>P)<sub>2</sub>W<sub>5</sub>, bipy and C<sub>6</sub>H<sub>5</sub>PO<sub>3</sub>H<sub>2</sub> have been detected at room temperature (Fig. S6<sup>†</sup>). From the result shown in Fig. S6b,<sup>†</sup> it is found that the TBA-(C<sub>6</sub>H<sub>5</sub>P)<sub>2</sub>W<sub>5</sub> shows luminescence with two main emission peaks at 380 nm and 470 nm with λ<sub>ex</sub> = 290 nm, attributing to LMCT (O → W). C<sub>6</sub>H<sub>5</sub>PO<sub>3</sub>H<sub>2</sub> and bipy display an emission peak at about 292 and 363 nm (λ<sub>ex</sub> = 290 nm), respectively, assigned to the intra-ligand π\* → π transition (Fig. S6c<sup>†</sup>). Compared with TBA-(C<sub>6</sub>H<sub>5</sub>P)<sub>2</sub>W<sub>5</sub>, compound **1** shows different luminescent property: two main broad emission bands at 400 and 470 nm with λ<sub>ex</sub> = 290 nm (Fig. S6a<sup>†</sup>), and the emissions of **1** are mainly caused

Fig. 5 The catalytic activity of **1** (a) and **2** (b) used after four runs

resulting from the coordination of {(C<sub>6</sub>H<sub>5</sub>P)<sub>2</sub>W<sub>5</sub>} to Cu<sup>2+</sup> ions.<sup>9</sup> Compound **2** shows emission peaks at 450 and 470 nm with λ<sub>ex</sub> = 290 nm (Fig. S6d<sup>†</sup>), compared with **1**, the peak shifts about 50 nm toward the longer wavelength.

#### Catalytic activity of two compounds

The carbonyl protection reaction is one of the very important organic reactions, and the acid catalyst plays a significant role in this reaction. The synthesis of cyclohexanone ethylene ketal was selected as a model reaction to research the acid catalytic activity of compounds **1** and **2** (Scheme S1<sup>†</sup>)<sup>10,11</sup>. In order to obtain the optimal catalytic conditions of the above target reaction, the effects of various factors including reaction time, amount of catalyst and molar ratio of cyclohexanone to glycol were systemically investigated and selected. Compound **1** as a representative example, the catalytic performances are presented in Figs. S7-9,<sup>†</sup> As seen from Figs. S7-9,<sup>†</sup> the optimum conditions for the synthesis of cyclohexanone ethylene ketal were as follows: the reaction time is 3.5 h, the molar ratio of the catalyst to cyclohexanone is 1:350 (that is, 0.06 mmol catalyst); the cyclohexanone/glycol molar ratio is 1:1.4; reaction temperature 95-100 °C, respectively. For comparing the catalytic activities of the as-synthesized compounds with the reference catalysts, the target reaction catalyzed by CuCl<sub>2</sub>, TBA-(C<sub>6</sub>H<sub>5</sub>P)<sub>2</sub>W<sub>5</sub>, bipy-Cu-(C<sub>6</sub>H<sub>5</sub>P)<sub>2</sub>Mo<sub>5</sub> (entries 2-4) was also performed under the optimum conditions, and the results were listed in Table 2. In addition, the reaction without any catalyst was also tested, and the yield of ketal was only 9% (entry 1). As exhibited in Table 2, it is found that compounds **1** and **2** showed high acid catalytic activity, and the yield of cyclohexanone ethylene ketal is 95% and 91%, respectively (entries 5 and 6). Obviously, compound **1** exhibit better catalytic activity than the parent TBA-(C<sub>6</sub>H<sub>5</sub>P)<sub>2</sub>W<sub>5</sub>, essentially, the Cu<sup>2+</sup> and W<sup>6+</sup> moieties, as the catalytically active center, play the most important roles in the catalytic reaction. Furthermore, the acid catalytic activity of compound **1** is higher than that of compound **2** slightly. The difference of catalytic activity of compounds **1** and **2** may derive from the difference of their structures. The former has an organophosphorus center in the structure, which may have a positive effect on acid catalytic activity of compound **1**. Furthermore, in comparison of compound **1** and bipy-Cu-(C<sub>6</sub>H<sub>5</sub>P)<sub>2</sub>Mo<sub>5</sub>, the dosage of **1** is less than that of bipy-Cu-(C<sub>6</sub>H<sub>5</sub>P)<sub>2</sub>Mo<sub>5</sub> at the same reaction condition, in other words, the catalytic activity of {(C<sub>6</sub>H<sub>5</sub>P)<sub>2</sub>W<sub>5</sub>} series is better than that of {(C<sub>6</sub>H<sub>5</sub>P)<sub>2</sub>Mo<sub>5</sub>} series. As shown in Fig. 5, compounds **1** and **2** can be reused three cycles without distinct decrease of the ketal yield in optimum reaction conditions. Especially, the

catalysts were recovered by simple filtration without any treatment. In summary, compounds **1** and **2** are efficient heterogeneous acid catalysts for the synthesis of cyclohexanone ethylene ketal reaction.

## Conclusions

In summary, a new Strandberg-type organophosphotungstate has been successfully assembled. Compound **1** represents the first example of transition metal introduced into the  $\{(RP)_2W_5\}$  series, which enriching the structural diversity of Strandberg-type POM family. The acquisition of compound **2**, from another point of view, illustrates that the synthetic conditions of  $\{(C_6H_5P)_2W_5\}$  series are generally harsher than the  $\{(C_6H_5P)_2Mo_5\}$  series, and many factors, such as pH and proportion of starting materials are all very important. Compared with the isostructural bipy-Cu(II)- $\{(C_6H_5P)_2Mo_5\}$  coordination polymer,<sup>2c</sup> compound **1** displays higher catalytic performance toward the synthesis of cyclohexanone ethylene ketal, and can be reused three cycles without significant deactivation. The solid-state luminescent study shows that compound **1** also displays good photoluminescence property.

## Acknowledgements

This work was financially supported by the Natural Science Foundation of Liaoning Province (no. 2013020128), the Foundation of Education Department of Liaoning Province (no. L2013414), National Natural Science Foundation of China (no. 21503103), the National Undergraduate Innovation and Entrepreneurship Training Program (no.201510165039) and Youth scientific research project of Liaoning Normal University (no. LS2014L018).

## Notes and references

- (a) E. D. Koutsouroubi, A. K. Xylouri and G. S. Armatas, *Chem. Commun.*, 2015, 51, 4481; (b) A. Macdonell, N. A. B. Johnson, A. J. Surman and L. Cronin, *J. Am. Chem. Soc.*, 2015, 137, 5662; (c) A. Parrot, G. Izzet, L. M. Chamoreau, A. Proust, O. Oms, A. Dolbecq, K. Hakouk, H. E. Bekkachi, P. Deniard, R. Dessapt and P. Mialane, *Inorg. Chem.* 2013, 52, 11156; (d) X. J. Sang, J. S. Li, L. C. Zhang, Z. M. Zhu, W. L. Chen, Y. G. Li, Z. M. Su and E. B. Wang, *Chem. Commun.*, 2014, 50, 14678; (e) J. Walsh, A. M. Bond, R. J. Forster and T. E. Keyes, *Coord. Chem. Rev.* 2016, 306, 217; (f) Z. L. Li, Y. Wang, L. C. Zhang, J. P. Wang, W. S. You and Z. M. Zhu, *Dalton Trans.*, 2014, 43, 5840.
- (a) R. C. Finn and J. Zubieta, *Inorg. Chem.*, 2001, 40, 2466; (b) T. M. Smith, K. Perkins, D. Symester, S. R. Freund, J. Vargas, L. Spinub and J. Zubieta, *CrystEngComm*, 2014, 16, 191; (c) J. P. Wang, H. X. Ma, L. C. Zhang, W. S. You and Z. M. Zhu, *Dalton Trans.*, 2014, 43, 17172.
- (a) C. R. Mayer and R. Thouvenot, *J. Chem. Soc.*, *Dalton Trans.*, 1998, 7; (b) R. C. Finn, R. S. Rarig, Jr. and J. Zubieta, *Inorg. Chem.*, 2002, 41, 2109; (c) A. Dolbecq, L. Lisnard, P. Mialane, J. Marrot, M. Bnard, M. M. Rohmer and F. Scheresse, *Inorg. Chem.*, 2006, 45, 5898; (d) G. Armatas, D. G. Allis, A. Prosvirin, G. Carnutu, C. J. O'Connor, K. Dunbar and J. Zubieta, *Inorg. Chem.*, 2008, 47, 832; (e) N. G. Armatas, W.

- Ouellette, K. Whitenack, J. Pelcher, H. X. Liu, E. Romaine, C. J. O'Connor and J. Zubieta, *Inorg. Chem.*, 2009, 48, 8897; (f) P. DeBurgomaster, A. Aldous, H. X. Liu, C. J. O'Connor and J. Zubieta, *Cryst. Growth Des.*, 2010, 10, 2209; (g) L. Yang, P. T. Ma, Z. Zhou, J. P. Wang and J. Y. Niu, *Inorg. Chem.*, 2013, 52, 8285.
- (a) P. DeBurgomaster, A. Aldous, H. X. Liu, C. J. O'Connor and J. Zubieta, *Cryst. Growth Des.*, 2010, 10, 5; (b) U. Kortz, C. Marquer, R. Thouvenot and M. Nierlich, *Inorg. Chem.*, 2003, 42, 1158; (c) E. Burkholder, V. Golub, C. J. O'Connor and J. Zubieta, *Inorg. Chem.*, 2004, 43, 7014.
- W. S. Kwak, M. T. Pope, in *Inorg. Synth.*, ed. A. P. Ginsberg, John Wiley & Sons, Inc., 1990, vol. 27, pp. 123
- G. M. Sheldrick, *Acta Crystallogr., Sect. A* 2008, 64, 112.
- G. M. Sheldrick, SADABS. Department of Structural Chemistry, University of Göttingen: Göttingen, Germany, 2008.
- B. Z. Lin, Z. Li, B. H. Xu, L. W. He, X. Z. Liu, C. Ding, *J. Mol. Struct.*, 2006, 825, 87.
- X. M. Li, Y. G. Chen, C. Su, S. Zhou, Q. Tang and T. Shi, *Inorg. Chem.*, 2013, 52, 11422.
- D. J. Tao, Z. M. Li, Z. Cheng, N. Hu and X. S. Chen, *Ind. Eng. Chem. Res.*, 2012, 51, 16263.
- J. H. Liu, X. F. Wei, Y. L. Yu, J. L. Song, X. Wang, A. Li, X. W. Liu and W. Q. Deng, *Chem. Commun.*, 2010, 46, 1670.

# Controllable assembly, characterization and catalytic property of a new Strandberg-type organophosphotungstate

Hong-Xin Ma,<sup>a</sup> Jing Du,<sup>a</sup> Fang Su,<sup>\*a,b</sup> Ting Lu,<sup>a</sup> Zai-Ming Zhu,<sup>\*a</sup> Lan-Cui Zhang<sup>\*a</sup>

## Graphic Abstract

A new Strandberg-type organophosphotungstate was assembled under hydrothermal condition and displayed good fluorescence property and catalytic activity.

